NEOPLASIA
www.neoplasia.com

Volume 14 Number 10 October 2012 pp. 893–904 893

Deubiquitinase USP9x Confers Radioresistance through Stabilization of Mcl-1[1,2]

Donatella Trivigno*, Frank Essmann†, Stephan M. Huber* and Justine Rudner*,‡

*Department of Radiation Oncology, University Hospital Tübingen, Tübingen, Germany; †Interfaculty Institute for Biochemistry, Eberhard Karls University, Tübingen, Germany; ‡Institute of Cell Biology, University Hospital Essen, Essen, Germany

Abstract

Myeloid cell leukemia sequence 1 (Mcl-1), an antiapoptotic member of the Bcl-2 family, is often overexpressed in tumor cells limiting the therapeutic success. Mcl-1 differs from other Bcl-2 members by its high turnover rate. Its expression level is tightly regulated by ubiquitylating and deubiquitylating enzymes. Interaction of Mcl-1 with certain Bcl-2 homology domain 3 (BH3)–only members of the Bcl-2 family can limit the access to Mcl-1 ubiquitin ligase E3 and stabilizes the antiapoptotic protein. In addition, the overexpression of the deubiquitinase ubiquitin-specific protease 9x (USP9x) can result in the accumulation of Mcl-1 by removing poly-ubiquitin chains from Mcl-1 preventing its proteasomal degradation. Analyzing radiation-induced apoptosis in Jurkat cells, we found that Mcl-1 was downregulated more efficiently in sensitive parental cells than in a resistant subclone. The decline of Mcl-1 correlated with cell death induction and clonogenic survival. Knockdown of BH3-only proteins Bim, Puma, and Noxa did not affect Mcl-1 level or radiation-induced apoptosis. However, ionizing radiation resulted in activation of USP9x and enhanced deubiquitination of Mcl-1 in the radioresistant cells preventing fast Mcl-1 degradation. USP9x knockdown enhanced radiation-induced decrease of Mcl-1 and sensitized the radioresistant cells to apoptosis induction, whereas USP9x knockdown alone did not change Mcl-1 level in unirradiated cells. Together, our results indicate that radiation-induced activation of USP9x inhibits Mcl-1 degradation and apoptosis resulting in increased radioresistance.

Neoplasia (2012) 14, 893–904

Introduction

The success of many antineoplastic therapies is based on a thorough removal of tumor cells through induction of apoptosis. Ionizing radiation that is commonly used in anticancer therapies and many cytotoxic drugs, e.g., anthracyclines, induces cell death through the mitochondrial pathway that is controlled by the Bcl-2 protein family. The family is subdivided into an antiapoptotic group consisting of Bcl-2 itself, Bcl-xL, and myeloid cell leukemia sequence 1 (Mcl-1) among others and a proapoptotic group. The latter comprises the multidomain proteins Bax, Bak, and Bok, as well as several Bcl-2 homology domain 3 (BH3)–only containing proteins [1]. The antiapoptotic members maintain mitochondrial integrity, prevent the release of proapoptotic factors from the intermembrane space into the cytosol and the subsequent caspase activation. In addition, the protective Bcl-2, Bcl-xL, and Mcl-1 are overexpressed in diverse tumors and constitute resistance factors that prevent a successful antitumor therapy [2,3]. Therefore, understanding the regulatory mechanisms of the antiapoptotic proteins is crucial for the success of future therapies.

The antiapoptotic proteins can interact with the BH3 domain of proapoptotic Bcl-2 members to neutralize each other [4]. Although all antiapoptotic Bcl-2 family members exhibit redundant protective function, they cannot always substitute each other [5–7]. Moreover,

Abbreviations: BH3, Bcl-2 homology domain 3; GSK-3β, glycogen synthase kinase-3β; IR, ionizing radiation; Mcl-1, myeloid cell leukemia sequence 1; Mule, Mcl-1 ubiquitin ligase E3; β-TrCP, β-transducin repeat–containing protein; USP9x, ubiquitin-specific protease 9x

Address all correspondence to: Justine Rudner, PhD, Institute of Cell Biology, University Hospital Essen, Virchowstr. 173, 45147 Essen, Germany. E-mail: justine.rudner@uk-essen.de

[1]The work was supported by grants from the German Research Foundation DFG (RU 1641/1-1) to J.R. and by the Wilhelm Sander Stiftung to S.M.H. (2011.083.1). The authors declare no conflict of interests.

[2]This article refers to supplementary material, which is designated by Figure W1 and is available online at www.neoplasia.com.

Received 29 March 2012; Revised 16 August 2012; Accepted 16 August 2012

DOI 10.1593/neo.12598

the protective proteins are regulated by distinct mechanisms at the transcriptional, translational, and posttranslational levels [8–10]. In contrast to Bcl-2 and Bcl-xL, Mcl-1 is a short-lived protein with a high turnover rate. Shutdown of protein translation results in a rapid decline [10]. Sequestration by BH3-only proteins and phosphorylation reportedly regulate Mcl-1 degradation [11–15]. Interestingly, different kinases can have opposite effect on the turnover of Mcl-1. Whereas phosphorylation by extracellular regulated kinases 1 and 2 (ERK1/2) at threonine 163 slows Mcl-1 protein turnover, phosphorylation at serine 159 by glycogen synthase kinase-3β (GSK-3β) targets Mcl-1 for ubiquitylation and proteasomal degradation [12,14]. The transfer of ubiquitin moieties is catalyzed by ubiquitin ligases. So far, three ubiquitin ligases targeting Mcl-1 were identified, namely, Mcl-1 ubiquitin ligase E3 (Mule), β-transducin repeat–containing protein (β-TrCP), and FBW7 [16–19]. β-TrCP and FBW7 are the Mcl-1–recognizing components of the Skip/Collin/F-box ubiquitin ligase complex. Previous publications indicate that phosphorylation of Mcl-1 accelerates β-TrCP– or FBW7-dependent degradation of the antiapoptotic protein [16,18]. The single peptide ligase Mule, in contrast, contains a BH3-like domain through which the enzyme interacts with Mcl-1 similar to the complex formed by Mcl-1 with other BH3-only proteins [19]. Consequently, Noxa—and probably also Bim and Puma—can limit the access of Mule and Mule-dependent degradation of Mcl-1 while interacting with the antiapoptotic protein [13,15].

The ubiquitylation can be reversed by deubiquitinases. Recently, the deubiquitinase ubiquitin-specific protease 9x (USP9x) was described to remove poly-ubiquitin chains from Mcl-1, thereby stabilizing the protective protein and increasing resistance to apoptosis induced by the Bcl-2/Bcl-xL inhibitor ABT-737 [20]. Increased USP9x expression correlates with Mcl-1 protein levels in human follicular and diffuse large B-cell lymphomas and is associated with poor prognosis for patients with multiple myeloma [20].

Despite the growing knowledge about the mechanisms controlling Mcl-1 stability, little is known how Mcl-1 levels are regulated in response to ionizing radiation (IR). Using Jurkat T lymphoma cells, we analyzed the sensitivity of two clones to IR-induced apoptosis. The sensitive cells died faster and exhibited a lower clonogenic survival upon irradiation than the resistant cells. In both clones, the radiosensitivity correlated with IR-induced Mcl-1 decline, and the reduction of Mcl-1 levels was prerequisite for apoptosis induction. Thus, the ability to maintain high Mcl-1 levels for a much longer time might explain the reduced radiosensitivity of the resistant cell clone. Interestingly, inhibition of GSK-3β could not prevent Mcl-1 degradation, suggesting that the kinase does not regulate Mcl-1 stability. To further analyze the mechanism controlling Mcl-1 turnover, BH3-only proteins Bim, Puma, and Noxa and the deubiquitinase USP9x were silenced by siRNA. However, knockdown of none of the BH3-only proteins affected the Mcl-1 level or IR-induced apoptosis.

IR induced activation of USP9x in resistant Jurkat cells 24 hours after irradiation. This activation coincided with an enhanced interaction between USP9x and Mcl-1 and enhanced Mcl-1 deubiquitylation. Accordingly, knockdown of USP9x accelerated the radiation-induced Mcl-1 degradation and sensitized the radioresistant Jurkat subclone and another tumor cell line, the radioresistant K562 chronic myelogenous leukemia cells, to apoptosis. We conclude that radioresistance can be acquired by activation of USP9x that stabilizes Mcl-1 protein levels and increases cell survival.

Materials and Methods

Reagents and Antibodies

Pan-caspase inhibitor zVAD-fmk was purchased from Bachem (Bubendorf, Switzerland), cycloheximide from Sigma (Deisenhofen, Germany), GSK-3 inhibitor XV and MG132 from Calbiochem (Merck, Darmstadt, Germany), and WP1130 from Selleck Chemicals (Munich, Germany).

The following antibodies were used for Western blot analysis and immunoprecipitation: mouse anti–caspase-9 and rabbit anti-Bak from Upstate (Millipore, Schwalbach, Germany), rabbit anti–caspase-3, poly (ADP ribose) polymerase (PARP), Mcl-1, Bcl-xL, β-catenin, GSK-3β, phospho–GSK-3β (S21/9), Akt, phospho-Akt (S473) and phospho-Akt (T308), and mouse anti-ubiquitin (clone P4D1) from Cell Signaling (NEB, Frankfurt, Germany), rabbit anti-Puma and Bim from Epitomics (Biomol, Hamburg, Germany), mouse anti–Bcl-2 from Santa Cruz Biotechnology (Heidelberg, Germany), mouse anti-Noxa from Calbiochem (Merck), rabbit anti-USP9x from Novus Biologicals and mouse anti-USP9x from Abnova (both distributed by Acris, Heford, Germany), mouse anti–Mcl-1 from Pharmingen (Becton Dickinson, Heidelberg, Germany), mouse anti–glyceraldehyde 3-phosphate dehydrogenase (GAPDH) from Abcam (Cambridge, United Kingdom), and mouse anti–β-actin from Sigma.

Cells and Cell Culture

Jurkat E6 T lymphoma cells (Jurkat-sensitive) and K562 chronic myelogenous leukemia cells were from ATCC (Bethesda, MD). The radioresistant Jurkat subclone emerged after a prolonged cell culture. Cells were grown in RPMI 1640 medium supplemented with 10% fetal calf serum (Gibco Life Technologies, Eggenstein, Germany) and maintained in a humidified incubator at 37°C and 5% CO_2.

Transfection with siRNA

Cells were cultured at a low density to ensure log phase growth. For transfection, 3×10^6 cells were resuspended in 300 μl of RPMI-1640 without phenol red. After adding siRNA at indicated concentrations, Jurkat cells were electroporated at 370 V for 10 ms and K562 cells at 340 V for 5 ms, using an EPI2500 electroporator (Fischer, Heidelberg, Germany). Immediately after transfection, cells were resuspended in prewarmed medium and continued to be cultured as described above. Transfection efficiency and viability were determined by transfecting the cells with 400-nM green fluorescence siGLO siRNA followed by propidium iodide exclusion dye and flow cytometric analysis. Mcl-1, Puma, Bim, Noxa, USP9x ON-TARGET SMARTpools, siCONTROL NON-TARGETING pool, and siGLO siRNA were purchased from Dharmacon (Chicago, IL).

Flow Cytometric Analysis

The mitochondrial membrane potential ($\Delta\Psi_m$) was analyzed using the $\Delta\Psi_m$-specific dye tetramethylrhodamine ethyl ester (Molecular Probes, Mobitech, Goettingen, Germany). At the indicated time points, cells were stained for 30 minutes in phosphate-buffered saline (PBS) containing 25 nM tetramethylrhodamine ethyl ester. To examine DNA fragmentation, we incubated cells with PBS containing 0.1% Triton X-100 and 10 μg/ml propidium iodide. Short-term survival was measured employing a propidium iodide exclusion dye. The cells were incubated with PBS containing 10 μg/ml propidium iodide in the absence of any detergent. Cells were detected in channel 2 employing a FACS Calibur flow cytometer (Becton Dickinson) and

analyzed with the FCS Express 3 software (De Novo Software, Los Angeles, CA). Data show mean values ± SD of at least six independent experiments.

Clonogenic Test

Clonogenic survival was analyzed as described before [21]. In brief, cells were seeded at different dilutions and irradiated with 0 to 8 Gy. For each dilution, the amount of wells that shows a repopulation 4 weeks after irradiation was counted. Using the Origin 6.0 software (Microcal Inc., Northampton, MA), the amount of cells that was needed to repopulate 50% of the wells (WC50) was calculated. The surviving fraction (SF) was calculated by normalizing the WC50 values of irradiated cells to the WC50 values of the respective nonirradiated control cells. The error of SF was calculated by error propagation according to Gauss.

Western Blot Analysis

Cells were lysed in 200 µl of lysis buffer containing 50 mM Hepes (pH 7.5), 150 mM NaCl, 1% Triton X-100, 1 mM EDTA, 10 mM sodium pyrophosphate, 10 mM NaF, 2 mM Na_3VO_4, 100 mM PMSF, 5 µg/ml aprotinin, 5 µg/ml leupeptin, and 3 µg/ml pepstatin. Protein was separated by sodium dodecyl sulfate–polyacrylamide gel electrophoresis (SDS-PAGE) under reducing conditions and transferred onto polyvinylidene fluoride (PVDF) membranes (Roth, Karlsruhe, Germany). Blots were blocked in TBS buffer containing 0.05% Tween 20 and 5% nonfat dry milk for 1 hour at room temperature. The membrane was incubated overnight at 4°C with the respective primary antibodies. The secondary antibody was incubated for 1 hour at room temperature. Detection of antibody binding was performed by enhanced chemiluminescence (ECL Western Blotting Analysis System; GE Healthcare/Amersham Biosciences, Freiburg, Germany). Equal loading was verified by antibodies against GAPDH or β-actin. Where indicated, protein levels were quantified by densitometry using the ImageJ software (ImageJ 1.40g, National Institutes of Health, Bethesda, MD). All Western blot experiments were repeated at least once.

Immunoprecipitation

Cells were lysed as described above using 1% CHAPS as detergent. The protein concentration was adjusted to 2 mg/ml. Two micrograms of anti-USP9x antibody (Novus Biologicals) or 10 µl of anti–Mcl-1 antibody (Cell Signaling) and 50 µl of slurry Dynabeads suspension (Dynal/Invitrogen, Karlsruhe, Germany) were added to 750 µl of lysate. After precipitation for 3 hours at 4°C, the beads were washed thrice with 300 µl of lysis buffer containing 0.2% of the respective detergent. Proteins were eluted by boiling the beads for 10 minutes in 100 µl of SDS sample buffer containing 2.5% β-mercaptoethanol. Thirty microliters of the eluate was separated by SDS-PAGE before transfer to PVDF membrane and detection by chemiluminescence as described above. Immunoprecipitations were repeated at least once.

Ubiquitin-7-amino-4-methylcoumarin (AMC) Assay

Cells were lysed in DUB buffer [20 mM Hepes (pH 7.5), 150 mM NaCl, 0.5% NP-40, and 5 mM $MgCl_2$]. Five hundred micrograms of protein was precipitated with 1 µg of rabbit anti-USP9x antibody as described above. Washed beads were suspended in 100 µl of DUB buffer. The reaction was started by adding 500 nM ubiquitin-AMC and detected with a Tecan microplate reader (Infinite 200, Tecan, Mainz, Germany) using excitation at 380 nm and emission at 460 nm. Six independent experiments were performed. Data represent mean values ± SD.

USP9x–Mcl-1 Assay

IR-resistant cells were irradiated with 0 or 10 Gy or treated with 5 µM MG132. Twenty-four hours after irradiation, cells were lysed in buffer containing 20 mM Hepes (pH 7.5), 150 mM NaCl, 1% CHAPS, and 5 mM $MgCl_2$. USP9x was precipitated as described above. Alternatively, cells treated with MG132 were lysed and Mcl-1 was precipitated from the lysates as described above. The precipitates were washed three times with a buffer containing 20 mM Hepes (pH 7.5), 150 mM NaCl, 0.2% CHAPS, and 5 mM $MgCl_2$ and resuspended in 20 µl of washing buffer additionally containing 50 µl of dithiothreitol (DTT). The precipitated Mcl-1 was added to the USP9x precipitates and incubated for 30 minutes at 37°C. Where indicated, USP9x activity was inhibited by adding 5 µM WP1130 before uniting with precipitated Mcl-1. Afterward, precipitates were separated by SDS-PAGE under reducing conditions and analyzed by Western blot using antibodies against ubiquitin, Mcl-1, and USP9x.

Mcl-1 Degradation Assay

Cells were treated with 1 µM cycloheximide for 0, 0.5, 1, 2, and 3 hours. At indicated time points, cells were lysed and lysates were separated as described above. Mcl-1 protein levels were detected by Western blot analysis. Several Western blots were made from the same lysates. Protein levels were quantified by densitometry using ImageJ software (ImageJ 1.40g, National Institutes of Health). Monoexponential decay was fitted using Origin 6.0 software and normalized as described in the legend.

Data Analysis

Statistical significance was calculated by a one-way analysis of variance (ANOVA) test using GraphPad Software (San Diego, CA).

Results

Effective Down-regulation of Mcl-1 Correlates with Radiosensitivity in Jurkat Lymphoma Cells

To analyze resistance mechanisms that prevent apoptosis induction in response to IR, we irradiated two clones of Jurkat T lymphoma cells with 10 Gy. Dissipation of the mitochondrial membrane potential ($\Delta\Psi_m$) and DNA degradation (sub-G1 population) were analyzed by flow cytometry (Figure 1, *A–D*). The clones differ in their sensitivity to radiation-induced apoptosis. $\Delta\Psi_m$ dissipation and DNA degradation occurred more efficiently in the IR-sensitive parental clone than in the IR-resistant subclone (Figure 1, *A–D*).

Furthermore, short-term survival upon irradiation with 10 Gy was analyzed employing a propidium iodide exclusion dye (Figure 1*E*), whereas long-term survival was examined by clonogenic assay using limiting cell dilutions to calculate the SF (Figure 1*F*). Both assays showed that the short-term as well as the long-term survival was lower in the IR-sensitive cells. The activation of the initiator caspase-9, the executioner caspase-3, and cleavage of caspase-3 substrate PARP were impaired in the resistant cells after irradiation (Figure 1*G*). The levels of the antiapoptotic Bcl-2 and Bcl-xL, as well as of the proapoptotic Bcl-2 family members Bak and Bim, remained unchanged in both cell clones. However, levels of the antiapoptotic Mcl-1 visibly decreased in the IR-sensitive cells, whereas levels of the specific Mcl-1 interacting BH3-only protein Noxa were unaffected (Figure 1*G*).

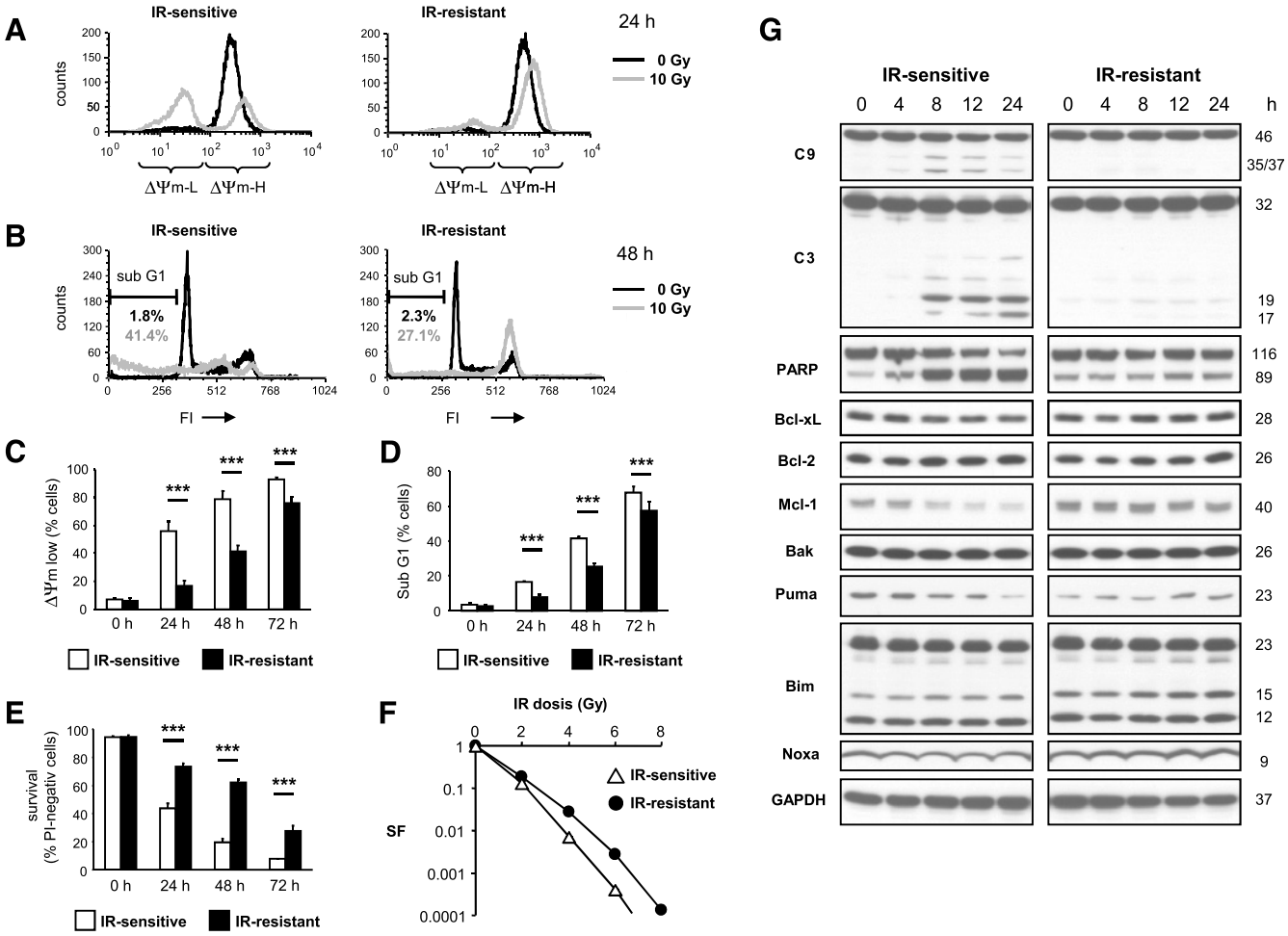

Figure 1. IR-induced down-regulation of Mcl-1 and apoptosis induction are impaired in resistant Jurkat subclone. Sensitive (IR-sensitive) and resistant (IR-resistant) Jurkat cells were irradiated with 10 Gy. $\Delta\Psi_m$ dissipation (A, C), DNA degradation (B, D), and survival (E) were analyzed by flow cytometry at indicated time points after irradiation. (A) Representative histograms show cells with intact ($\Delta\Psi_m$-H for high $\Delta\Psi_m$) and dissipated ($\Delta\Psi_m$-L for low $\Delta\Psi_m$) mitochondrial membrane potential 24 hours after irradiation. (B) Representative histograms display cells with degraded DNA visualized in the sub-G1 fraction 48 hours after irradiation. Results of $\Delta\Psi_m$ dissipation and DNA fragmentation are shown in C and D, respectively ($n = 6$, mean ± SD). Radiation-induced $\Delta\Psi_m$ dissipation and DNA fragmentation were significantly reduced in IR-resistant cells. (E) Cell death and survival were quantified by flow cytometry employing a propidium iodide exclusion dye ($n = 8$, mean ± SD). (F) Long-term survival was analyzed in a clonogenic assay using limiting dilutions of the IR-resistant and IR-sensitive cells. The SF was calculated for cells irradiated with 0, 2, 4, 6, and 8 Gy (normalized to respective nonirradiated cells). Error bars of SF are within the symbols. (G) Western blot analysis shows cleavage of caspase-9, caspase-3, and the caspase-3 substrate PARP in sensitive cells in response to IR, which is abrogated in resistant cells. Down-regulation of Mcl-1 and Puma levels are detected in IR-sensitive cells only. Levels of other Bcl-2 proteins (Bcl-xL, Bcl-2, Bak, Bim, and Noxa) were not affected by irradiation. GAPDH was used as loading control. ***$P < .001$.

To clarify the importance of Mcl-1 down-regulation for mitochondrial permeabilization and apoptosis induction, we electroporated nontargeting (nt) or Mcl-1–targeting (mcl1) siRNA into both clones. Mcl-1 levels were reduced by the specific siRNA already 3 hours after electroporation and not detectable 3 more hours later (Figure 2*A*). Consistent with Mcl-1 decline, $\Delta\Psi_m$ dissipated within 6 hours after electroporation (Figure 2*B*), indicating the pivotal function of Mcl-1 in maintenance of mitochondrial homeostasis and cell survival in both Jurkat clones.

GSK-3β Does Not Control Mcl-1 Stability in Jurkat Cells

Because Mcl-1 is essential for Jurkat cell survival, we set out to analyze the mechanisms regulating its protein levels. Mcl-1 function and stability can be controlled by BH3-only proteins, by kinases like GSK-3β, by ubiquitin ligases facilitating proteasomal degradation, and by deubiquitinases preventing proteasomal degradation.

First, we analyzed the regulation of Mcl-1 by GSK-3β. The kinase GSK-3β is inactive when phosphorylated by PKB/Akt, thus unable to phosphorylate and destabilize Mcl-1. Interestingly, IR had no impact on phospho-Akt and phospho–GSK-3β in Jurkat cells, even though Mcl-1 and β-catenin levels decreased (Figure 3*A*). To test whether GSK-3β influences radiation-induced apoptosis, we treated IR-sensitive cells with 30 nM GSK-3 inhibitor XV when irradiated with 10 Gy. Treatment with GSK-3 inhibitor XV resulted in an accumulation of the GSK-3β target β-catenin without changing Mcl-1 levels or IR-induced Mcl-1 decline (Figure 3*B*). Flow cytometric analysis showed that $\Delta\Psi_m$ dissipation (Figure 3*C*) and DNA degradation (Figure 3*D*) occurred to the same extent in inhibitor- or vehicle-treated cells.

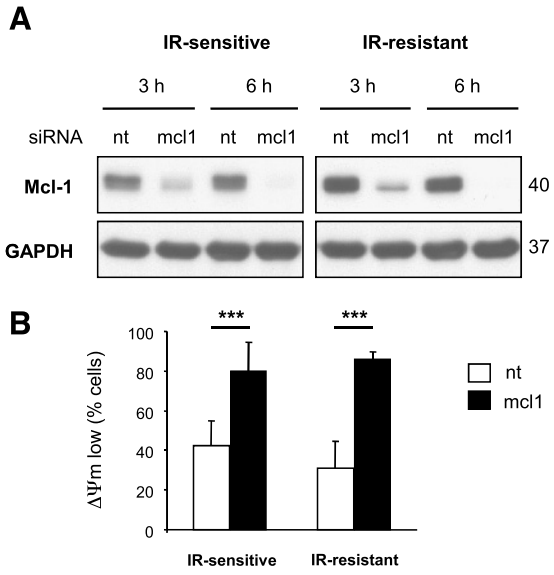

Figure 2. Mcl-1 prevents mitochondrial permeabilization in IR-sensitive and IR-resistant cells. Mcl-1 siRNA (mcl1; 500 nM) or nontargeting siRNA (nt) was electroporated into IR-sensitive and IR-resistant Jurkat cells. (A) Three and six hours after electroporation, lysates were made, and down-regulation of Mcl-1 was analyzed by Western blot analysis. GAPDH was used as loading control. (B) Six hours after electroporation, dissipation of mitochondrial membrane potential ($\Delta\Psi_m$ low) was analyzed by flow cytometry. In both IR-sensitive and IR-resistant cells, the expression of Mcl-1 is essential for maintaining mitochondrial homeostasis. ***$P < .001$.

Furthermore, phosphorylation of Mcl-1 could not be detected in irradiated or nonirradiated Jurkat cells (Figure W1*B*). From those experiments, we conclude that the PKB/Akt–GSK-3β pathway does not regulate Mcl-1 levels in Jurkat cells.

BH3-only Proteins Are Not Involved in Mcl-1 Stability

Our next focus was on those BH3-only proteins, which are known interaction partners of Mcl-1. Bim, Puma, and Noxa were described to be upregulated in response to irradiation. In our cell system, however, Bim and Noxa levels remained unchanged (Figure 1*G*), whereas Puma levels decreased 24 hours after irradiation in IR-sensitive cells. Cotreatment of those cells with the pan-caspase inhibitor zVAD abrogated the decline of Puma but not of Mcl-1 (Figure 4*A*), indicating that change of Puma levels occurred in the executive phase of apoptosis after caspase activation, whereas Mcl-1 was downregulated before caspases became activated (Figures 1*G* and 4*A*).

The association of the BH3-only proteins with Mcl-1 might change during radiation-induced apoptosis independent of their protein levels. We, therefore, silenced the expression of Bim, Puma, and Noxa by siRNA in the sensitive clone. Down-regulation of respective proteins was verified by Western blot analysis 72 hours after electroporation (Figure 4, *B–D*, *upper panels*). Two days after electroporation, cells were irradiated with 10 Gy. $\Delta\Psi_m$ dissipation (Figure 4, *B–D*, *middle panels*) and DNA degradation (Figure 4, *B–D*, *lower panels*) were analyzed 24 and 48 hours after irradiation, respectively. Surprisingly, silencing of Bim, Puma, or Noxa did not alter Mcl-1 protein levels, radiation-induced $\Delta\Psi_m$ dissipation, and DNA degradation. The results indicate that none of the three BH3-only proteins regulates radioresistance in the Jurkat cells.

USP9x Controls Mcl-1 Stability in Jurkat Lymphoma Cells

In previous publications, USP9x was shown to interact with Mcl-1 and β-catenin [20,22]. Both proteins were downregulated only in

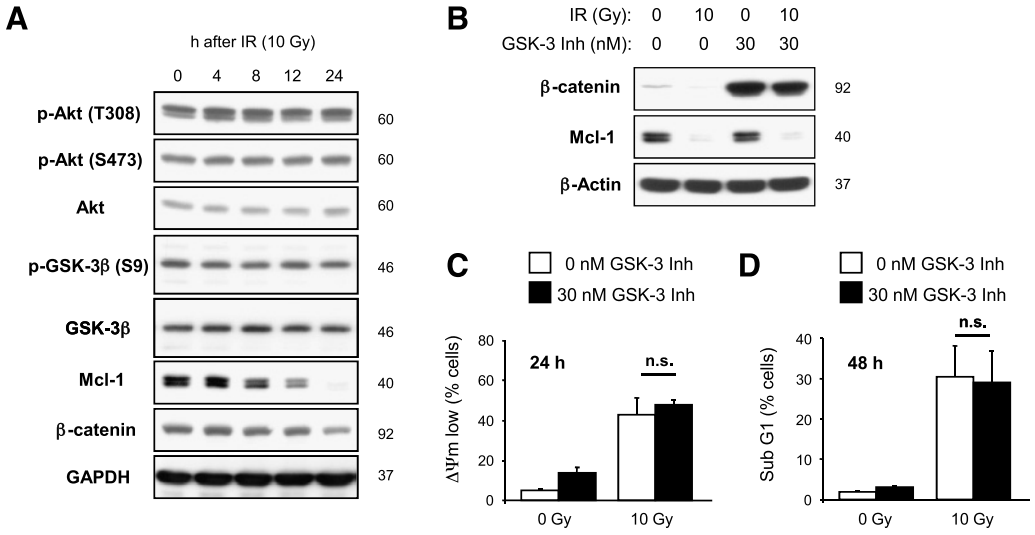

Figure 3. GSK-3β does not regulate Mcl-1 stability in irradiated Jurkat cells. (A) IR-sensitive Jurkat cells were irradiated with 10 Gy. Cells were lysed 24 hours after irradiation. Western blot analysis shows that phopsho–GSK-3β levels were not changed by IR, whereas the levels of GSK-3β substrates Mcl-1 and β-catenin were clearly reduced. (B–D) IR-sensitive Jurkat cells were irradiated with 10 Gy in the presence of 30 nM GSK-3 inhibitor XV. (B) Twenty-four hours later, cells were lysed and analyzed by Western blot. Treatment of IR-sensitive Jurkat cells with 30 nM GSK-3 inhibitor XV for 24 hours resulted in an accumulation of β-catenin without having an effect on Mcl-1 levels. GSK-3 inhibitor XV did not alter a radiation-induced Mcl-1 decline. Dissipation of mitochondrial membrane potential ($\Delta\Psi_m$) was analyzed by flow cytometry 24 hours after irradiation. (D) DNA fragmentation was analyzed by flow cytometry 48 hours after irradiation. GSK-3 inhibitor XV had no effect on radiation-induced $\Delta\Psi_m$ dissipation or DNA degradation. Flow cytometric data show means ± SD ($n = 6$); NS indicates no significance ($P > .05$).

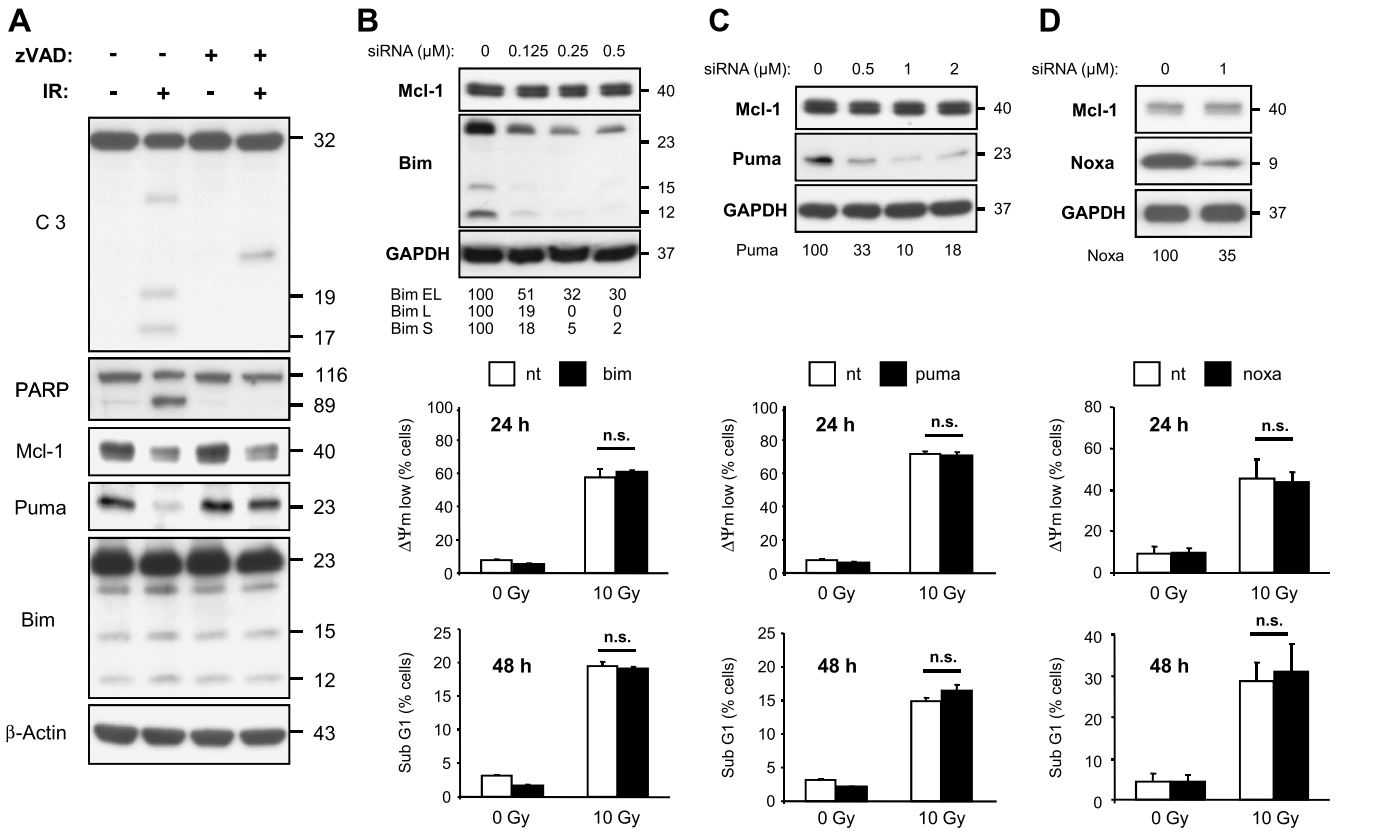

Figure 4. Bim, Puma, and Noxa are dispensable for radiation-induced apoptosis. (A) IR-sensitive Jurkat cells were treated with 30 μM caspase inhibitor zVAD or the solvent only and irradiated with 10 Gy. Twenty-four hours later, cell lysates were made and analyzed by Western blot analysis. Radiation-induced decline of Puma but not of Mcl-1 could be blocked by the caspase inhibitor, indicating that down-regulation of Mcl-1 occurs upstream of caspase activation, whereas Puma is downregulated after caspase activation. (B) Bim siRNA (500 nM), (C) Puma siRNA (1 μM), (D) Noxa siRNA (1 μM), or respective concentrations of nontargeting (nt) siRNA were electroporated into IR-sensitive Jurkat cells. Forty-eight hours later, cells were irradiated with 10 Gy. $\Delta\Psi_m$ dissipation was examined 24 hours after irradiation by flow cytometry (B–D, middle panels), whereas DNA fragmentation was analyzed 48 hours after irradiation (B–D, lower panels). Data show means ± SD (n = 3); NS indicates no significance ($P > .05$). Down-regulation of Bim, Puma, and Noxa and Mcl-1 levels were verified by Western blot analysis 72 hours after electroporation (B and C, upper panels). The knockdown of the respective proteins was quantified by densitometry. Abrogation of Bim, Puma, or Noxa expression did not affect radiation-induced apoptosis in Jurkat cells.

IR-sensitive but not in IR-resistant cells after irradiation (Figure 5*A*). In contrast, USP9x levels were not changed in both, IR-sensitive and IR-resistant cells, in response to IR. However, USP9x, when activated, might specifically enhance its affinity to Mcl-1 and remove the ubiquitin chains from Mcl-1, thereby stabilizing the antiapoptotic protein in IR-resistant cells. To test this hypothesis, we precipitated Mcl-1 from IR-sensitive and IR-resistant cells before and 24 hours after irradiation with 10 Gy. Much more USP9x coprecipitated with Mcl-1 in irradiated resistant cells than in the nonirradiated control cells (Figure 5*B*). On the contrary, this radiation-induced increased association of USP9x and Mcl-1 could not be detected in IR-sensitive cells.

To test whether the half-life time of Mcl-1 was altered in irradiated cells, IR-sensitive and IR-resistant cells were treated with 1 μM cycloheximide 24 hours after irradiation with 10 Gy. Densitometric analysis of Mcl-1 levels in Western blot shows that, in response to IR, Mcl-1 half-life time was greatly decreased in sensitive cells but not in resistant cells (Figure 5, *C–E*). This indicates that an enhanced degradation rate accelerates Mcl-1 decline in IR-sensitive cells following irradiation.

An enhanced association of USP9x with Mcl-1 does not necessarily reflect an enhanced USP9x enzymatic activity. Thus, we performed a fluorometric activity assay following precipitation of USP9x from irradiated and nonirradiated control cells. Notably, a significant increase of USP9x activity could be detected only in IR-resistant but not in IR-sensitive cells 24 hours after irradiation (Figure 6*A*). Using a pan–phospho-serine/threonine antibody, we also detected an IR-induced phosphorylation of USP9x, which was markedly higher in the IR-resistant than in IR-sensitive cells indicating a posttranslational modification in response to IR (Figure W1*A*).

Moreover, when adding purified ubiquitylated Mcl-1 to precipitated USP9x, we could detect a decrease of ubiquitylated, high molecular Mcl-1 and an accumulation of p40 Mcl-1, indicating an Mcl-1 deubiquitylation by USP9x following irradiation. Mcl-1 deubiquitylation was much more pronounced when incubated with USP9x precipitated from irradiated IR-resistant cells compared with USP9x precipitated from nonirradiated IR-resistant cells (Figure 6*B*, *left and middle lane*). Inhibition of USP9x activity by WP1130 (5 μM) prevented deubiquitylation of Mcl-1 in irradiated IR-resistant cells (Figure 6*B*, *right lane*).

In addition, analysis of ubiquitylated protein by Western blot following Mcl-1 precipitation shows less ubiquitylated, high molecular Mcl-1 in IR-resistant cell 24 hours after irradiation than in nonirradiated

control cells (Figure 6*C*). Such a decrease of ubiquitylated, high molecular Mcl-1 was not observed in IR-sensitive cells 24 hours after irradiation. Interestingly, an overall change of ubiquitylated proteins, such as is observed 3 hours after treatment with 5 μM proteasome inhibitor MG132, could not be detected in Jurkat cells 24 hours after irradiation with 10 Gy (Figure 6*D*), indicating a specific regulation of Mcl-1 ubiquitylation status following irradiation.

USP9x Knockdown Sensitizes Radioresistant Cells to IR-induced Apoptosis

The observation was also supported in the next set of experiments in which USP9x was downregulated by siRNA. USP9x knockdown was verified 48 hours after electroporation with 1 μM nontargeting or USP9x-targeting siRNA. Interestingly, depletion of USP9x did not affect Mcl-1 levels in IR-sensitive or IR-resistant cells (Figure 7*A*). Forty-eight hours after electroporation, IR-sensitive and IR-resistant cells were irradiated with 10 Gy. Twenty-four and forty-eight hours after irradiation, $\Delta\Psi_m$ (Figure 7*B*) and cellular DNA content (Figure 7*C*) were analyzed by flow cytometry. USP9x knockdown slightly, but significantly, enhanced $\Delta\Psi_m$ dissipation and DNA degradation in IR-sensitive cells. The increase of $\Delta\Psi_m$ dissipation and DNA degradation was even more pronounced in the resistant subclone. In addition, Mcl-1 levels and caspase-3 activation were analyzed by Western blot (Figure 7*D*). To this end, IR-sensitive cells were lysed 24 hours and IR-resistant cells 30 hours after irradiation. A clear down-regulation of Mcl-1 and caspase-3 as well as PARP processing were observed in IR-sensitive Jurkat cells 24 hours after irradiation, whereas only a weak Mcl-1 decline and processed caspase-3 and PARP fragments were detected in the IR-resistant subclone 30 hours after irradiation. Silencing of USP9x hardly accelerated IR-induced Mcl-1 degradation and caspase-3 processing in the IR-sensitive cells 24 hours after irradiation. In contrast, USP9x silencing clearly accelerated the decline of Mcl-1 as well as caspase-3 activation and PARP cleavage in IR-resistant cells 30 hours after irradiation, although Mcl-1 down-regulation and caspase-3 activation did not reach the same extent as in the IR-sensitive clone. To examine the effect of USP9x knockdown on Mcl-1 degradation in IR-resistant cells, the half-life time was analyzed 48 hours after irradiation with 10 Gy (Figure 7, *E*–*G*). Although irradiation alone reduced slightly, but not significantly, Mcl-1 half-life, USP9x knockdown resulted in a further significant reduction of Mcl-1 half-life. Our results indicate that USP9x stabilizes Mcl-1 upon irradiation in the resistant Jurkat subclone, whereas it has no effects on Mcl-1 in nonirradiated cells.

To exclude an effect limited to our Jurkat cell model, we examined the role of USP9x in radiation-induced apoptosis in another cell line. Irradiation with 10 Gy hardly induced caspase-3 activation and PARP cleavage within the first 48 hours in K562 cells, a chronic myelogenous leukemia cell line (Figure 8*A*). A decrease of Mcl-1 levels was observed not until 48 hours after irradiation. Therefore, hardly any DNA fragmentation was detected until 72 hours after irradiation (Figure 8*B*). Obviously, K562 cells are very refractory to radiation-induced apoptosis. Silencing of USP9x by siRNA significantly enhanced DNA degradation 72 hours after irradiation (Figure 8*C*) and also accelerated Mcl-1 decline as well as caspase-3 and PARP processing (Figure 8*D*). Thus, the radioprotective effects of USP9x were observed not only in radioresistant Jurkat cells but also in

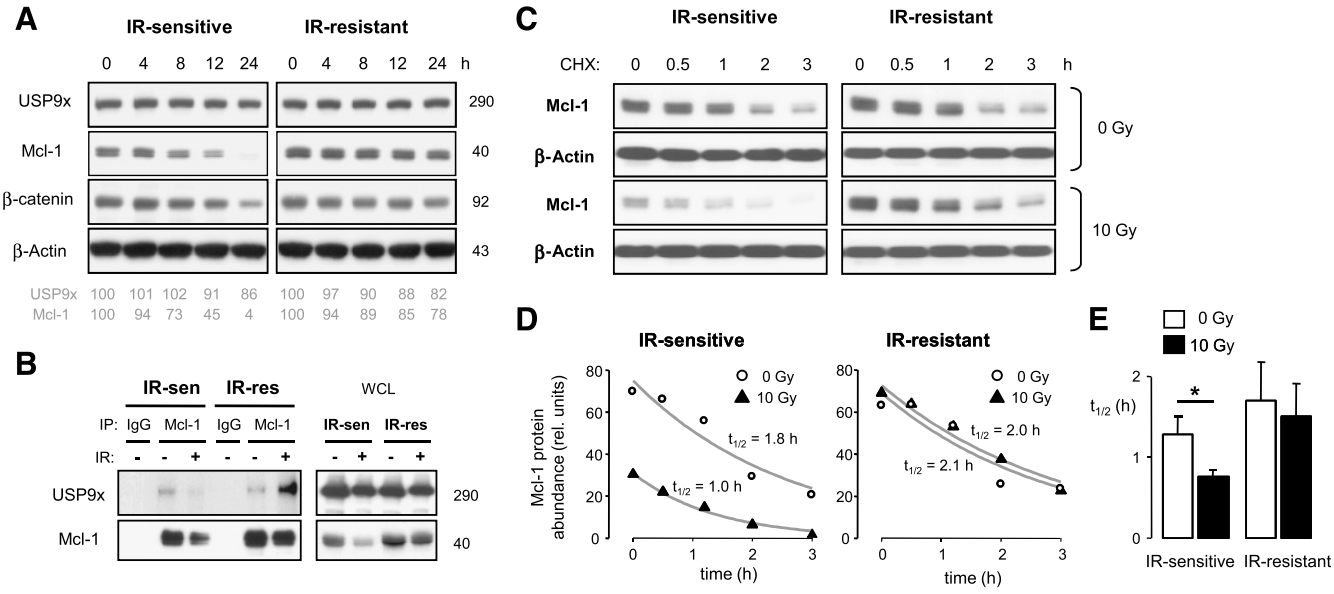

Figure 5. Irradiation enhances interaction of Mcl-1 with USP9x in resistant cells and prevents Mcl-1 degradation. (A) IR-sensitive and IR-resistant Jurkat cells were irradiated with 10 Gy. Lysates were made 4, 8, 12, and 24 hours later and analyzed by Western blot. USP9x levels did not change in response to irradiation. The levels of potential USP9x substrates Mcl-1 and β-catenin decreased only in IR-sensitive cells upon irradiation. Densitometric quantification of USP9x and Mcl-1 is shown below the Western blots of the respective cells. (B) IR-sensitive and IR-resistant cells were irradiated with 10 Gy. Twenty-four hours later, Mcl-1 was precipitated from irradiated and nonirradiated cells. More USP9x coprecipitated in irradiated IR-resistant than in IR-sensitive cells. The whole-cell lysate (WCL) shows the overall Mcl-1 and USP9x protein levels before precipitation. (C–E) Twenty-four hours after irradiation with 10 Gy, cells were treated with 1 μM cycloheximide (CHX) for 0 to 3 hours. Cells were lysed at respective time points. (C) Mcl-1 levels were analyzed by Western blot. (D) Mcl-1 levels were quantified by densitometry. The values were fitted and the half-life of Mcl-1 was calculated. (E) Graph shows the mean values ± SD of Mcl-1 half-life time ($n = 7$). *$P < .05$.

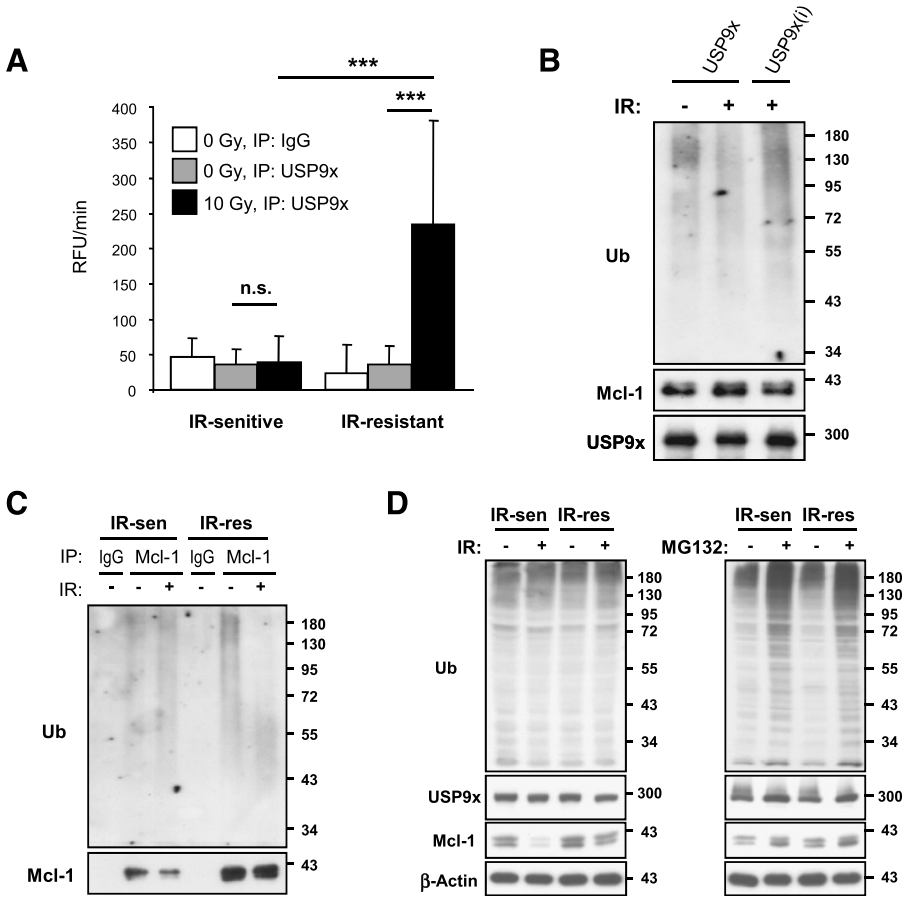

Figure 6. Ionizing radiation induces activation of USP9x and deubiquitylation of Mcl-1 in IR-resistant cells. (A) IR-sensitive and IR-resistant Jurkat cells were irradiated with 10 Gy. Twenty-four hours after irradiation, USP9x was precipitated from the lysates. (A) The activity of USP9x was determined by adding a fluorogenic substrate to the precipitated USP9x. Increased USP9x activity could be detected only in resistant cells 24 hours after irradiation. Data show mean values ± SD ($n = 6$); ***$P < .001$; NS indicates no significance ($P > .05$). (B) IR-resistant Jurkat cells were irradiated with 10 Gy. Twenty-four hours after irradiation, USP9x was precipitated from the lysates of irradiated and nonirradiated control cells. In parallel, IR-resistant cells were treated with 5 μM proteasome inhibitor MG132 for 3 hours to accumulate ubiquitylated Mcl-1. To start the deubiquitylation reaction, we added ubiquitylated Mcl-1 precipitated from MG132-treated lysates to the USP9x precipitated from irradiated lysates. Mcl-1 deubiquitylation was analyzed by Western blot using an antibody against ubiquitin and Mcl-1. Where indicated by (i), USP9x activity was inhibited by adding 5 μM WP1130 before the incubation with precipitated Mcl-1. Less ubiquitylated Mcl-1 and more p40 Mcl-1 were detected after incubation with USP9x precipitated from irradiated cells. (C) Twenty-four hours after irradiation with 10 Gy, Mcl-1 was precipitated from the lysates of irradiated or nonirradiated control cells. The ubiquitylation state of Mcl-1 was detected by Western blot using antibodies against ubiquitin and Mcl-1. IR-induced decrease of high molecular, ubiquitylated Mcl-1 was detected only in IR-resistant cells 24 hours after irradiation. (D) IR-sensitive and IR-resistant Jurkat cells were either irradiated with 10 Gy (left panel) or treated with 5 μM MG132 (right panel). Cell lysates were analyzed by Western blot. No change of ubiquitylated proteins in WCLs was observed 24 hours after irradiation. In contrast, treatment with MG132 for 3 hours resulted in an accumulation of ubiquitylated proteins as well as USP9x and Mcl-1.

radioresistant K562 cells, indicating a more general mechanism of radioresistance mediated by USP9x.

Taken together, our findings suggest a novel mechanism of radioresistance that involves the activation of the deubiquitinase USP9x and the USP9x-dependent stabilization of Mcl-1 following irradiation.

Discussion

Failure to Downregulate Mcl-1 Mediates Radioresistance

Ionizing radiation is widely used in antitumor therapies because of its antiproliferative and cytotoxic effects. The response to irradiation varies profoundly between different tumors. Factors responsible for radioresistance need to be identified and targeted to improve the therapeutical outcome. The related proteins Bcl-2, Bcl-xL, and Mcl-1 are already identified as radioresistance factors [23–27]. When overexpressed, they prevent radiation-induced apoptosis, enhance survival, and impair tumor response to radiotherapy. In our present study, we focused on Mcl-1 whose stability is tightly regulated by ubiquitin ligases and deubiquitinases. For the first time, we could show that the deubiquitinase USP9x contributes to radioresistance by stabilizing Mcl-1 protein levels.

To identify a molecular mechanism regulating radioresistance, we used two Jurkat lymphoma cell clones that differ in their radiosensitivity, which arose spontaneously after prolonged cell culture. IR-induced apoptosis was delayed in resistant cells. In addition, short-term as well as long-term survival was significantly lower in sensitive cells upon radiation. Interestingly, the down-regulation of Mcl-1 protein levels in response to IR occurred faster in sensitive cells.

The survival of both cell clones depended on Mcl-1 because down-regulation of Mcl-1 by siRNA resulted in a rapid mitochondrial permeabilization and thus in cell death. We, therefore, concluded that the failure of efficient Mcl-1 down-regulation was probably responsible for enhanced survival or the IR-resistant cells following irradiation. Those results support an earlier observation that IR-induced depletion of Mcl-1 correlated with radiation-induced apoptosis [28]. Other experiment, however, indicate that apoptosis can proceed without Mcl-1 degradation [29]. Thus, we cannot exclude the involvement of other factors controlling the radiosensitivity in Jurkat cells.

Many tumors exceedingly overexpress Mcl-1 and fail to down-regulate the protective protein in response to single drug treatment, underlining the importance to reduce Mcl-1 half-life time to increase therapeutic success [30,31]. We detected decreased Mcl-1 turnover in sensitive Jurkat cells 24 hours after irradiation, whereas Mcl-1 half-life time was not significantly changed in resistant cells. Several possible mechanisms controlling Mcl-1 stability were described so far including the binding to BH3-only proteins, phosphorylation by kinases, and the regulation of its ubiquitylation status by ubiquitin ligases and deubiquitinases.

Regulation of Mcl-1 Stability and Radioresistance by BH3-only Proteins and Ubiquitin Ligases

Several recent publications indicate that BH3-only proteins Bim, Puma, and Noxa can destabilize Mcl-1 [11,13,32]. All three proteins are important mediators of radiation-induced apoptosis [33–35]. The mechanism is thought to involve the tumor suppressor p53 that upregulates the transcription of Bim, Puma, and Noxa in response to IR-induced DNA damage [33,35–38]. However, because of a mutation, Jurkat cells do not express p53 [39], thus an up-regulation of Bim, Puma, and Noxa was not observed in response to IR. Interestingly, Jurkat cells express the three BH3-only proteins even when not irradiated. Thus, a p53-independent mechanism has to regulate the expression of Bim, Puma, and Noxa in Jurkat cells. Although involved in IR-induced apoptosis in

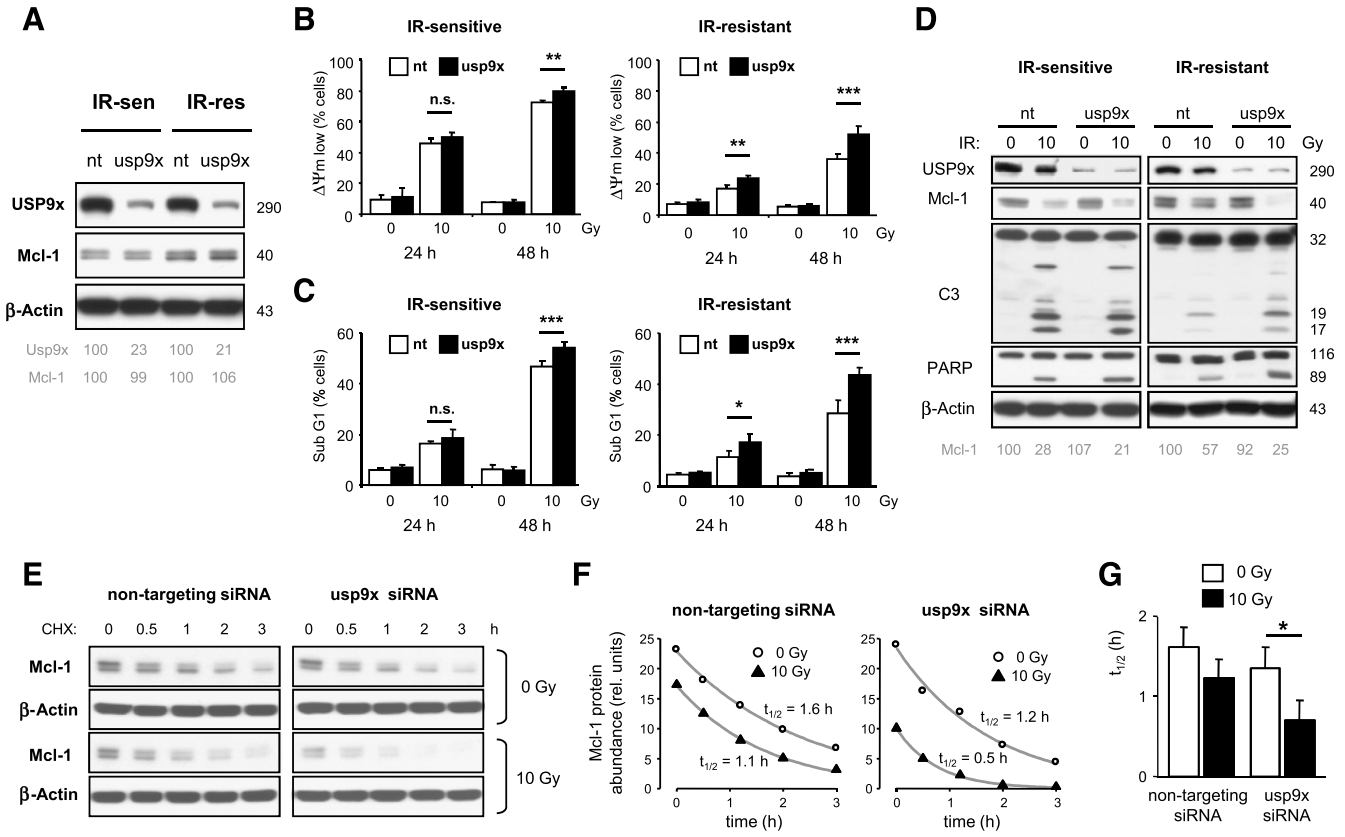

Figure 7. Depletion of USP9x enhances radiation-induced Mcl-1 degradation. Nontargeting (nt; 1 μM) or USP9x-targeting (usp9x) siRNA was electroporated into IR-sensitive and IR-resistant cells. (A) Forty-eight hours later, down-regulation of USP9x and Mcl-1 levels were examined by Western blot and quantified by densitometry. USP9x knockdown has no effect on Mcl-1 levels. (B–F) Forty-eight hours after electroporation, cells were irradiated with 10 Gy. $\Delta\Psi_m$ dissipation (B) and DNA fragmentation (C) were measured 24 and 48 hours after irradiation, respectively. Down-regulation of USP9x slightly enhanced radiation-induced $\Delta\Psi_m$ dissipation and DNA degradation in IR-sensitive cells. The sensitization was even greater in IR-resistant cells. Flow cytometric data show means ± SD (n = 6). *P < .05, **P < .01, ***P < .001; NS indicates no significance. (D) Forty-eight hours after electroporation, cells were irradiated with 10 Gy. Cells were lysed at indicated times after irradiation. Mcl-1 levels as well as caspase-3 and PARP processing were analyzed by Western blot. In addition, Mcl-1 levels were quantified by densitometry. IR-induced Mcl-1 decline, caspase-3 (C3), and PARP processing were clearly accelerated by USP9x silencing in IR-resistant cells 30 hours after irradiation (right panel). USP9x silencing in IR-sensitive cells did not alter Mcl-1 decline, caspase-3, and PARP processing 24 hours after irradiation (left panel). (E–G) Forty-eight hours after irradiation with 10 Gy, IR-resistant cells transfected with nt or usp9x siRNA were treated with 1 μM cycloheximide for 0 to 3 hours. Cells were lysed at respective time points. (E) Mcl-1 levels were analyzed by Western blot. (F) Mcl-1 levels were quantified by densitometry. The values were fitted and the half-life of Mcl-1 was calculated. (G) Graph shows the mean values ± SD of Mcl-1 half-life time (n = 4).

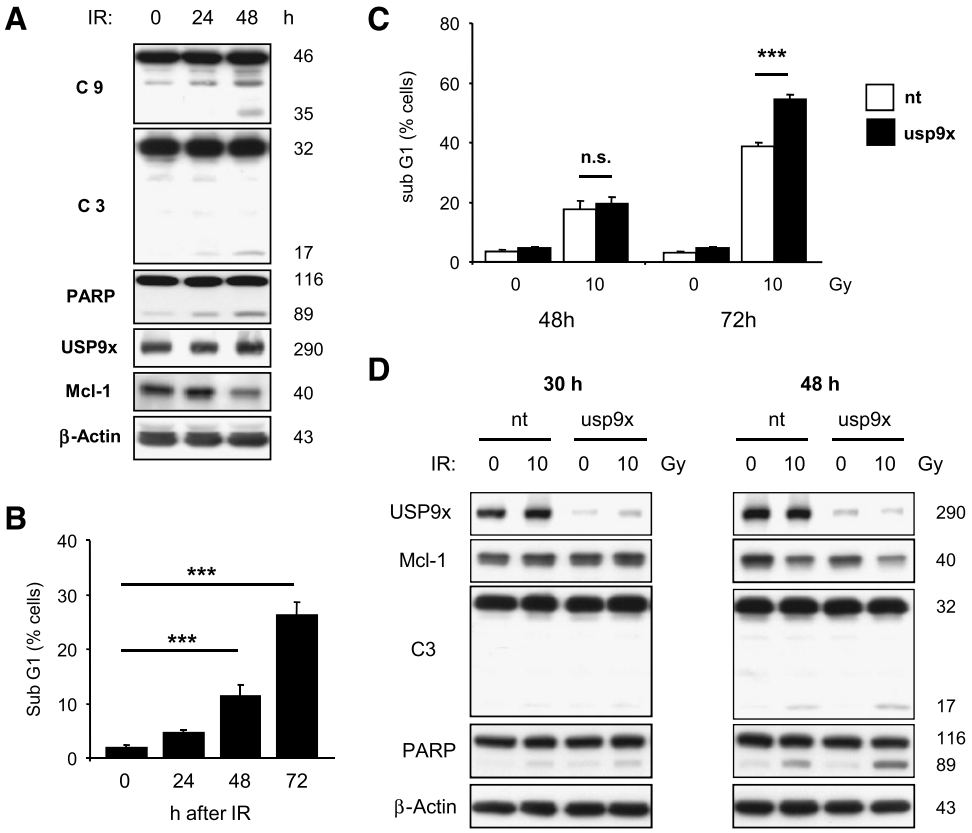

Figure 8. Silencing of USP9x accelerates Mcl-1 decline and apoptosis in IR-resistant K562 cells. K562 leukemic cells were irradiated with 10 Gy. (A) Cells were lysed 24 and 48 hours after irradiation. Western blot analysis shows weak caspase-9 (C9), caspase-3 (C3), and PARP cleavage, as well as Mcl-1 depletion, 48 hours after irradiation. (B) Flow cytometric analysis of DNA fragmentation indicates very moderate apoptosis induction within the first 48 hours after irradiation, which increased 72 hours after irradiation. (C, D) siRNA (1 μM) was electroporated into K562 cells. Forty-eight hours after electroporation, cells were irradiated with 10 Gy. (C) DNA fragmentation was analyzed 48 and 72 hours after irradiation. (D) Lysates were made 30 and 48 hours after irradiation. Down-regulation of USP9x enhanced Mcl-1 decline, as well as caspase-3 (C3) and PARP processing, 48 hours after irradiation. Flow cytometric data show means ± SD ($n = 6$). *** indicates high significance ($P < .001$); NS indicates no significance.

several cell types, knockdown experiments show that none of the three BH3-only proteins is essential for IR-induced apoptosis in Jurkat cells. In addition, we have shown that none of the proteins affects Mcl-1 levels. Thus, regulation of Mcl-1 levels by ubiquitin ligase Mule that competitively binds to Noxa is also very unlikely. Taken together, our results suggest that the BH3-only proteins do not regulate Mcl-1 stability and Jurkat cell survival upon irradiation.

Previous studies repeatedly reported that phosphorylation of Mcl-1 by GSK-3β can enhance its ubiquitylation and proteasomal degradation [16–18]. However, inhibition of GSK-3β did not change Mcl-1 levels or sensitivity to IR-induced apoptosis. Moreover, IR-induced phosphorylation of Mcl-1 could not be detected (see Figure W1). Although phosphorylation of Mcl-1 can accelerate its degradation, it is not essential for β-TrCP– or FBW7-dependent Mcl-1 degradation [16,18]. Thus, Skip/Collin/F-box ubiquitin ligases containing specific Mcl-1–recognizing components, such as β-TrCP or FBW7, might still control Mcl-1 turnover in Jurkat cells. Further experiments are needed to resolve the role of ubiquitin ligases in Mcl-1 degradation and radiosensitivity.

Regulation of Mcl-1 Stability by Deubiquitinases

Poly-ubiquitin chains can be removed from proteins by deubiquitinases, thereby preventing proteasomal degradation and stabilizing protein levels. A recent publication by Schwickart et al. has shown that down-regulation of USP9x increased the sensitivity to apoptosis induced by the Bcl-2 inhibitor ABT-737 and delayed tumor growth in xenograft mouse model [20]. From these experiments, Schwickart et al. concluded that the Mcl-1 turnover rate and tumor growth depended on USP9x expression. Our results indicate that changed Mcl-1 turnover is also responsible for altered responsiveness to IR. The radiosensitive and radioresistant Jurkat cells, however, expressed similar amounts of USP9x. Thus, the mere USP9x expression cannot explain the difference in radiosensitivity. However, radiosensitivity clearly depended on USP9x, because down-regulation of USP9x by siRNA increased radiosensitivity in the IR-resistant Jurkat and K562 cells. In contrast to earlier observations made by Schwickart et al., USP9x knockdown did not significantly change Mcl-1 protein levels or its turnover rate in nonirradiated cells. However, Mcl-1 half-life time was greatly reduced after irradiation when USP9x was silenced in the resistant subclone. The accelerated Mcl-1 decline correlates with enhanced apoptosis induction. Obviously, USP9x is an important factor that maintains Mcl-1 stability and survival upon irradiation. IR reduced also the half-life time of Mcl-1 in resistant cells transfected with nontargeting siRNA, although only slightly and not significantly. This indicates that, apart from USP9x, other factors contribute to Mcl-1 protein stability. This assumption is also

supported by Western blot analysis of IR-resistant Jurkat and K562 cells. Despite an excellent down-regulation of USP9x, IR-induced Mcl-1 decrease and caspase-3 activation did not occur to the same extent as in IR-sensitive Jurkat cells.

In the present study, we provide a link between USP9x activity, Mcl-1 stability, and radiosensitivity. USP9x becomes activated only in the resistant subclone 24 hours after IR and coincides with less ubiquitylated Mcl-1. In addition, USP9x precipitated from irradiated resistant cells was able to deubiquitylate Mcl-1 *in vitro*. Interestingly, IR-induced accumulation of ubiquitylated proteins in whole-cell lysates was not observed. Therefore, our results suggest a specific regulation of Mcl-1 protein levels in response to IR rather than a global shutdown of protein degradation.

So far nothing is known about the regulation of USP9x activity. USP9x becomes phosphorylated in response to IR (Figure W1*A*). Phosphorylation is often associated with changed enzymatic activity. Indeed, phosphorylation of USP9x correlated with enzymatic activity in irradiated Jurkat cells, but a direct link between phosphorylation and USP9x activation remains to be shown.

Taken together, we identified the deubiquitinase USP9x as a novel factor mediating radioresistance, which was activated in resistant cells upon irradiation and inhibited apoptosis induction by stabilizing Mcl-1 levels.

Acknowledgments

We thank Dr Frank Grünebach for providing the electroporation device and Heidrun Faltin for technical assistance.

References

[1] Youle RJ and Strasser A (2008). The BCL-2 protein family: opposing activities that mediate cell death. *Nat Rev Mol Cell Biol* **9**, 47–59.

[2] Adams JM and Cory S (2007). The Bcl-2 apoptotic switch in cancer development and therapy. *Oncogene* **26**, 1324–1337.

[3] Kelly PN and Strasser A (2011). The role of Bcl-2 and its pro-survival relatives in tumourigenesis and cancer therapy. *Cell Death Differ* **18**, 1414–1424.

[4] Chen L, Willis SN, Wei A, Smith BJ, Fletcher JI, Hinds MG, Colman PM, Day CL, Adams JM, and Huang DC (2005). Differential targeting of prosurvival Bcl-2 proteins by their BH3-only ligands allows complementary apoptotic function. *Mol Cell* **17**, 393–403.

[5] Rudner J, Elsaesser SJ, Jendrossek V, and Huber SM (2011). Anti-apoptotic Bcl-2 fails to form efficient complexes with pro-apoptotic Bak to protect from Celecoxib-induced apoptosis. *Biochem Pharmacol* **81**, 32–42.

[6] Rudner J, Elsaesser SJ, Muller AC, Belka C, and Jendrossek V (2010). Differential effects of anti-apoptotic Bcl-2 family members Mcl-1, Bcl-2, and Bcl-xL on celecoxib-induced apoptosis. *Biochem Pharmacol* **79**, 10–20.

[7] Willis SN, Chen L, Dewson G, Wei A, Naik E, Fletcher JI, Adams JM, and Huang DC (2005). Proapoptotic Bak is sequestered by Mcl-1 and Bcl-xL, but not Bcl-2, until displaced by BH3-only proteins. *Genes Dev* **19**, 1294–1305.

[8] Allen JC, Talab F, Zuzel M, Lin K, and Slupsky JR (2011). c-Abl regulates Mcl-1 gene expression in chronic lymphocytic leukemia cells. *Blood* **117**, 2414–2422.

[9] Deng X, Gao F, Flagg T, and May WS Jr (2004). Mono- and multisite phosphorylation enhances Bcl2's antiapoptotic function and inhibition of cell cycle entry functions. *Proc Natl Acad Sci USA* **101**, 153–158.

[10] Huber S, Oelsner M, Decker T, zum Buschenfelde CM, Wagner M, Lutzny G, Kuhnt T, Schmidt B, Oostendorp RA, Peschel C, et al. (2011). Sorafenib induces cell death in chronic lymphocytic leukemia by translational down-regulation of Mcl-1. *Leukemia* **25**, 838–847.

[11] Czabotar PE, Lee EF, van Delft MF, Day CL, Smith BJ, Huang DC, Fairlie WD, Hinds MG, and Colman PM (2007). Structural insights into the degradation of Mcl-1 induced by BH3 domains. *Proc Natl Acad Sci USA* **104**, 6217–6222.

[12] Domina AM, Vrana JA, Gregory MA, Hann SR, and Craig RW (2004). MCL1 is phosphorylated in the PEST region and stabilized upon ERK activation in viable cells, and at additional sites with cytotoxic okadaic acid or taxol. *Oncogene* **23**, 5301–5315.

[13] Gomez-Bougie P, Menoret E, Juin P, Dousset C, Pellat-Deceunynck C, and Amiot M (2011). Noxa controls Mule-dependent Mcl-1 ubiquitination through the regulation of the Mcl-1/USP9X interaction. *Biochem Biophys Res Commun* **413**, 460–464.

[14] Maurer U, Charvet C, Wagman AS, Dejardin E, and Green DR (2006). Glycogen synthase kinase-3 regulates mitochondrial outer membrane permeabilization and apoptosis by destabilization of MCL-1. *Mol Cell* **21**, 749–760.

[15] Warr MR, Acoca S, Liu Z, Germain M, Watson M, Blanchette M, Wing SS, and Shore GC (2005). BH3-ligand regulates access of MCL-1 to its E3 ligase. *FEBS Lett* **579**, 5603–5608.

[16] Ding Q, He X, Hsu JM, Xia W, Chen CT, Li LY, Lee DF, Liu JC, Zhong Q, Wang X, et al. (2007). Degradation of Mcl-1 by β-TrCP mediates glycogen synthase kinase 3-induced tumor suppression and chemosensitization. *Mol Cell Biol* **27**, 4006–4017.

[17] Inuzuka H, Shaik S, Onoyama I, Gao D, Tseng A, Maser RS, Zhai B, Wan L, Gutierrez A, Lau AW, et al. (2011). SCF(FBW7) regulates cellular apoptosis by targeting MCL1 for ubiquitylation and destruction. *Nature* **471**, 104–109.

[18] Wertz IE, Kusam S, Lam C, Okamoto T, Sandoval W, Anderson DJ, Helgason E, Ernst JA, Eby M, Liu J, et al. (2011). Sensitivity to antitubulin chemotherapeutics is regulated by MCL1 and FBW7. *Nature* **471**, 110–114.

[19] Zhong Q, Gao W, Du F, and Wang X (2005). Mule/ARF-BP1, a BH3-only E3 ubiquitin ligase, catalyzes the polyubiquitination of Mcl-1 and regulates apoptosis. *Cell* **121**, 1085–1095.

[20] Schwickart M, Huang X, Lill JR, Liu J, Ferrando R, French DM, Maecker H, O'Rourke K, Bazan F, Eastham-Anderson J, et al. (2010). Deubiquitinase USP9X stabilizes MCL1 and promotes tumour cell survival. *Nature* **463**, 103–107.

[21] Rudner J, Belka C, Marini P, Wagner RJ, Faltin H, Lepple-Wienhues A, Bamberg M, and Budach W (2001). Radiation sensitivity and apoptosis in human lymphoma cells. *Int J Radiat Biol* **77**, 1–11.

[22] Murray RZ, Jolly LA, and Wood SA (2004). The FAM deubiquitylating enzyme localizes to multiple points of protein trafficking in epithelia, where it associates with E-cadherin and β-catenin. *Mol Biol Cell* **15**, 1591–1599.

[23] An J, Chervin AS, Nie A, Ducoff HS, and Huang Z (2007). Overcoming the radioresistance of prostate cancer cells with a novel Bcl-2 inhibitor. *Oncogene* **26**, 652–661.

[24] Nix P, Cawkwell L, Patmore H, Greenman J, and Stafford N (2005). Bcl-2 expression predicts radiotherapy failure in laryngeal cancer. *Br J Cancer* **92**, 2185–2189.

[25] Skvara H, Thallinger C, Wacheck V, Monia BP, Pehamberger H, Jansen B, and Selzer E (2005). Mcl-1 blocks radiation-induced apoptosis and inhibits clonogenic cell death. *Anticancer Res* **25**, 2697–2703.

[26] Streffer JR, Rimner A, Rieger J, Naumann U, Rodemann HP, and Weller M (2002). BCL-2 family proteins modulate radiosensitivity in human malignant glioma cells. *J Neurooncol* **56**, 43–49.

[27] Wang J, Wakeman TP, Lathia JD, Hjelmeland AB, Wang XF, White RR, Rich JN, and Sullenger BA (2010). Notch promotes radioresistance of glioma stem cells. *Stem Cells* **28**, 17–28.

[28] Kubota Y, Kinoshita K, Suetomi K, Fujimori A, and Takahashi S (2007). Mcl-1 depletion in apoptosis elicited by ionizing radiation in peritoneal resident macrophages of C3H mice. *J Immunol* **178**, 2923–2931.

[29] Lee EF, Czabotar PE, van Delft MF, Michalak EM, Boyle MJ, Willis SN, Puthalakath H, Bouillet P, Colman PM, Huang DC, et al. (2008). A novel BH3 ligand that selectively targets Mcl-1 reveals that apoptosis can proceed without Mcl-1 degradation. *J Cell Biol* **180**, 341–355.

[30] Sieghart W, Losert D, Strommer S, Cejka D, Schmid K, Rasoul-Rockenschaub S, Bodingbauer M, Crevenna R, Monia BP, Peck-Radosavljevic M, et al. (2006). Mcl-1 overexpression in hepatocellular carcinoma: a potential target for antisense therapy. *J Hepatol* **44**, 151–157.

[31] Wirth T, Kuhnel F, Fleischmann-Mundt B, Woller N, Djojosubroto M, Rudolph KL, Manns M, Zender L, and Kubicka S (2005). Telomerase-dependent virotherapy overcomes resistance of hepatocellular carcinomas against chemotherapy and tumor necrosis factor-related apoptosis-inducing ligand by elimination of Mcl-1. *Cancer Res* **65**, 7393–7402.

[32] Mei Y, Du W, Yang Y, and Wu M (2005). Puma*Mcl-1 interaction is not sufficient to prevent rapid degradation of Mcl-1. *Oncogene* **24**, 7224–7237.

[33] Erlacher M, Michalak EM, Kelly PN, Labi V, Niederegger H, Coultas L, Adams JM, Strasser A, and Villunger A (2005). BH3-only proteins Puma and Bim are rate-limiting for gamma-radiation– and glucocorticoid-induced apoptosis of lymphoid cells *in vivo*. *Blood* **106**, 4131–4138.

[34] Michalak EM, Villunger A, Adams JM, and Strasser A (2008). In several cell types tumour suppressor p53 induces apoptosis largely via Puma but Noxa can contribute. *Cell Death Differ* **15**, 1019–1029.

[35] Oda E, Ohki R, Murasawa H, Nemoto J, Shibue T, Yamashita T, Tokino T, Taniguchi T, and Tanaka N (2000). Noxa, a BH3-only member of the Bcl-2 family and candidate mediator of p53-induced apoptosis. *Science* **288**, 1053–1058.

[36] Garrison SP, Phillips DC, Jeffers JR, Chipuk JE, Parsons MJ, Rehg JE, Opferman JT, Green DR, and Zambetti GP (2012). Genetically defining the mechanism of Puma- and Bim-induced apoptosis. *Cell Death Differ* **19**, 642–649.

[37] Nakano K and Vousden KH (2001). PUMA, a novel proapoptotic gene, is induced by p53. *Mol Cell* **7**, 683–694.

[38] Yu J, Zhang L, Hwang PM, Kinzler KW, and Vogelstein B (2001). PUMA induces the rapid apoptosis of colorectal cancer cells. *Mol Cell* **7**, 673–682.

[39] Vigorito E, Plaza S, Mir L, Mongay L, Vinas O, Serra-Pages C, and Vives J (1999). Contributions of p53 and PMA to gamma-irradiation induced apoptosis in Jurkat cells. *Hematol Cell Ther* **41**, 153–161.

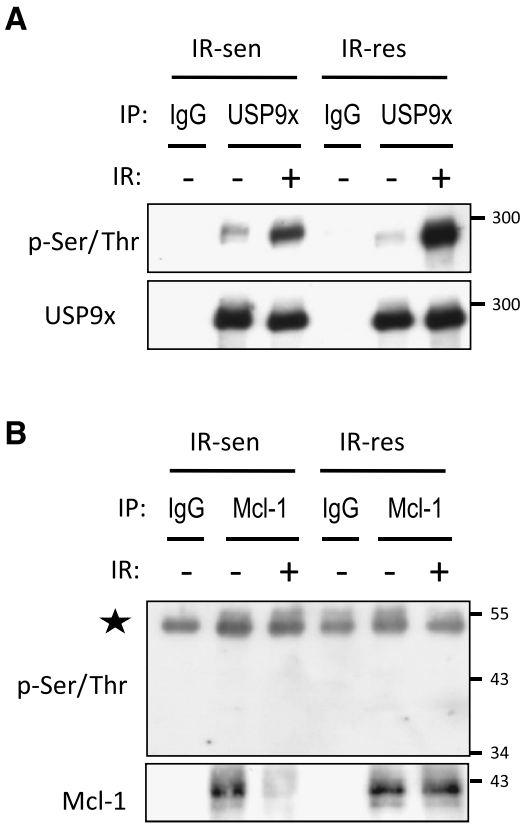

Figure W1. Irradiation induces phosphorylation of USP9x but not of Mcl-1. IR-sensitive and IR-resistant Jurkat cells were irradiated with 10 Gy. Twenty-four hours after irradiation, cells were lysed. (A) USP9x or (B) Mcl-1 was precipitated from the lysates. Using a phospho-Ser/Thr–specific antibody, radiation-induced phosphorylation of USP9x is detected by Western blot. IR-induced phosphorylation of USP9x is much higher in irradiated IR-resistant cells than IR-sensitive cells. In contrast, no phosphorylation of Mcl-1 could be detected. The star indicates an unspecific cross reactivity of the anti–phospho-Ser/Thr antibody with the rabbit antibody used to precipitate Mcl-1.